

Inhibition of Pitting Corrosion of the Stainless Steel by Dipyridinium Salts

A.Y. OBAID, S.A. AL-THABAATI, A.H. QUSTI and A.A. HERMAS*

¹Department of Chemistry, Faculty of Science, King Abdulaziz University, Jeddah, Saudi Arabia

²Department of Chemistry, Faculty of Science, Assiut University, Assiut, Egypt

*Corresponding author: Fax: +966 2 6952292; Tel: +966 2 6751355; E-mail: hagag_99@yahoo.com

(Received: 20 March 2012;

Accepted: 14 January 2013)

AJC-12693

The inhibitive actions of three sensitized derivatives of N,N'-diquaternized 4,4'-dipyridinium salts (TMdPyBr₂, HMdPyBr₂ and MPhdPyCl₂) on general and pitting corrosion of the stainless steel (SS) in aerated 0.1 M HCl have been studied at different temperatures. Corrosion potential and polarization measurements proved that the three compounds act as mixed type inhibitors with dominant anodic and their adsorption on the steel surface obey Langmuir adsorption isotherm. The diquaternized salts inhibited the corrosion and improved the passivation of the stainless steel, their inhibition efficiencies (except for TMdPyBr₂) increased with temperature. Electrochemical impedance measurements and optical microscopic investigation confirmed the inhibitive actions of these compounds and proved that both TMdPyBr₂ and HMdPyBr₂ inhibit the pitting initiation while MPhdPyCl₂ is less efficient inhibitor against the pitting. The mechanism of corrosion inhibition was discussed in the light of the molecular structure of the dipyridinium salts.

Key Words: Adsorption, Dipyridinium salts, Corrosion inhibition, Stainless steel, EIS.

INTRODUCTION

Stainless steels belong to a class of metal and alloys which protect themselves by forming passive film on their surface. However, in an environment with the presence of chloride ions, localized corrosion such as pitting and crevice corrosion is still a serious problem for this type of steel. For this reason, the research study for the passive film of stainless steels and their stability particularly in chloride solutions has a technological importance¹.

The use of inhibitor is one of the most practical methods for protection of different metals and alloys^{2,3} against the corrosion but few compounds can be applied usefully against the pitting corrosion⁴. The mechanism of corrosion inhibition by organic molecules is mostly attributed due to their adsorption onto metallic surfaces. The adsorption phenomenon depends, principally, on the chemical composition and structure of the inhibitors, nature of the metallic surface and the acidic properties of the medium where the inhibitor-surface interaction takes place⁵.

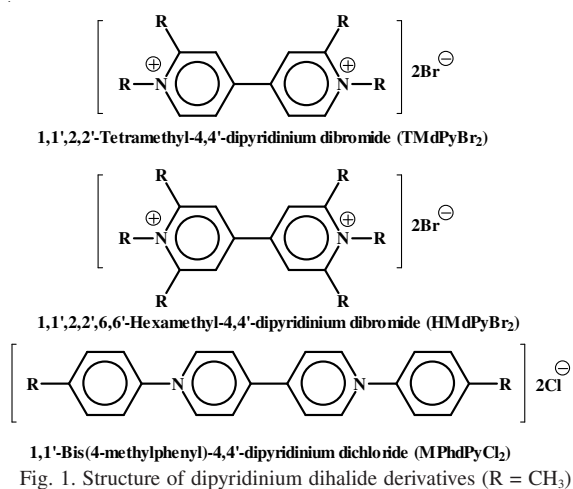
Surfactants, which consist of one polar group (hydrophilic) and one hydrophobic moiety have been used for several occasions by a large number of investigators and reported that surfactants acts as a good corrosion inhibitors⁶⁻¹⁴. Popova *et al.*^{6,7}, investigated four quaternary ammonium bromides of different heterocyclic compounds as corrosion inhibitors of mild steel in 1 M HCl and 1 M H₂SO₄. Viologens (N,N'-

diquaternized 4,4'-dipyridinium salts), which have been employed as herbicides, redox mediators, electrochromic materials, electron-transfer quenchers and as redox probes in self-assembled monolayers^{15,16}, could be used as efficient corrosion inhibitors^{17,18}. However, the details of dipyridinium dihalides role in the corrosion of stainless steel are not yet known. The purpose of this article is to investigate the effect of three substituted dipyridinium dihalides on the pitting corrosion of the stainless steel in acidic chloride medium. Potentiodynamic polarization, electrochemical impedance (EIS) measurements and optical microscopic investigation were employed.

EXPERIMENTAL

Three dipyridinium dihalide derivatives with chemical structure as shown in Fig. 1 were synthesized as described elsewhere¹⁸. A standard corrosion glass cell was used for the polarization and impedance measurements. The material of the working electrode is a sheet with area 1 cm² from ferritic type 430 stainless steel, it was cut from cold rolled annealed sheet (produced by Nilaco, Japan and containing 17-18.5 % chromium and < 1500 ppm carbon). The counter and reference electrodes are platinum sheet and silver-silver chloride (Ag/AgCl, saturated KCl), respectively.

General procedure: Prior to each experiment the working electrode was wet polished with emery papers up to grade 600, rinsed with bi-distilled water, acetone, bi-distilled water



and left in air for 0.5 h. Then, it was transferred to the glass cell which was filled by 200 mL of 0.1 M HCl solution. The electrolyte solution was prepared from concentrated analytical reagent HCl and bi-distilled water. The inhibitor solution was prepared by dissolving the appropriate weight in 0.1 M HCl solution. All experiments were conducted thermostatically at a given temperature and in an aerated condition without stirring.

Detection method: Electrochemical experiments were recorded using a potentiostat of type Autolab PGSTAT30, coupled to a computer equipped with GPES software for potential and polarization measurements and FRA software for EIS measurement. Potentiodynamic measurements were performed with 0.001 V s^{-1} . EIS measurements were conducted potentiostatically at open circuit potential (E_{cor}) with 10 mV rms with frequency range 50 kHz to 0.1 Hz. Microscopic investigation of the electrode surface in absence and presence of the inhibitor was performed by ZEISS optical microscope of type Stemi 2000-C and connected with Digital Canon Camera and computer.

RESULTS AND DISCUSSION

Corrosion potential measurement: After immersion the working electrode in the polarization cell, E_{cor} was recorded

versus time for *ca.* 0.5 h. The average value for E_{cor} of the stainless steel in 0.1 M HCl at 30 °C was 0.508 V (Ag/AgCl). The shifts of E_{cor} from the blank value caused by various concentrations of the studied compounds are shown in Table-1. Addition of any inhibitor from the three investigated compounds caused systematic displacement of the potential in the anodic direction, indicating that the anodic reaction is somewhat more inhibited than the cathodic reaction. The shift of E_{cor} at any concentration increased in the order $\text{MPhdPyCl}_2 < \text{TMdPyBr}_2 < \text{HMdPyBr}_2$.

Polarization measurement: Cathodic polarization and anodic polarization to a potential slightly more positive than the primary passive potential (E_{pp}) were carried out in 0.1 M HCl at 30 °C and in presence of various concentrations (5×10^{-5} - 1×10^{-3} M) of the inhibitors. Fig. 2 shows representative polarization curves in the absence and presence of HMdPyBr₂. Values of corrosion current density (i_{cor}) associated with the polarization curves were calculated by extrapolation of both anodic and cathodic branches (within Tafel regions) back to E_{cor} . The critical current density (i_{crit}) which corresponds to the E_{pp} was also obtained. It is a criterion for surface oxide formability on the stainless steel. The estimated parameters were recorded in Table-1. Although the positive shift of E_{cor} , both anodic and cathodic branches shifted to lower current density by addition of the inhibitors indicating inhibition of both the cathodic and anodic reactions. The investigated compounds most likely are mixed type inhibitors with dominant anodic, particularly for HMdPyBr₂. The shifting in the polarization curves runs parallel to that of the blank solution. So that, the addition of inhibitor may does not alter the mechanism of either hydrogen evolution or steel dissolution. It was also observed that these inhibitors decreased significantly i_{crit} and didn't affect on E_{pp} of the steel except slight positive shift at high concentrations of HMdPyBr₂ and MPhdPyCl₂.

From the i_{cor} values the inhibition efficiency (IE) of the additives was calculated according to:

$$\text{IE} = \left\{ \frac{[i_{\text{cor}}^{\circ} - i_{\text{cor}}]}{i_{\text{cor}}^{\circ}} \right\} \times 100 \quad (1)$$

where i_{cor}° and i_{cor} are corrosion current densities in the absence and presence of the inhibitor, respectively. By replacing

TABLE-1
EFFECT OF INHIBITOR CONCENTRATION ON THE POLARIZATION PARAMETERS

Inhibitor	Solution (M)	bc (mV/decade)	ba (mV/decade)	$-E_{\text{cor}}$ (V)	i_{cor} ($\mu\text{A cm}^{-2}$)	$-E_{\text{pp}}$ (V)	i_{crit} ($\mu\text{A cm}^{-2}$)
	Pure	90	62	508	599	417	2568
TMdPyBr ₂	5.0×10^{-5}	125	60	0.503	384	0.421	1887
	1.0×10^{-4}	130	48	0.492	244	0.418	1740
	2.5×10^{-4}	118	50	0.490	221	0.414	1635
	5.0×10^{-4}	112	38	0.486	194	0.431	1479
	1.0×10^{-3}	115	40	0.483	174	0.412	1289
HMdPyBr ₂	5.0×10^{-5}	115	66	0.495	511	0.415	2452
	1.0×10^{-4}	143	64	0.492	340	0.410	1369
	2.5×10^{-4}	105	45	0.484	226	0.415	1560
	5.0×10^{-4}	128	40	0.480	142	0.400	1307
	1.0×10^{-3}	111	38	0.472	172	0.405	1284
MPhdPyCl ₂	5.0×10^{-5}	137	65	0.505	397	0.411	2033
	1.0×10^{-4}	121	63	0.501	292	0.407	1732
	2.5×10^{-4}	114	66	0.498	246	0.387	1704
	5.0×10^{-4}	101	50	0.492	220	0.405	1537
	1.0×10^{-3}	93	58	0.493	240	0.406	1582

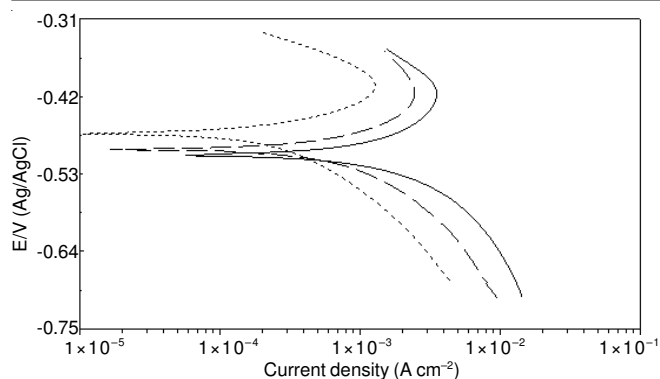


Fig. 2. Cathodic-anodic polarization for the SS in 0.1 M HCl (-) at 30 °C and in presence of 5×10^{-5} M (- -) and 1×10^{-3} M (· · ·) HMDPyBr₂

i_{cor} with i_{crit} in the above equation suppression efficiency (SE) of the additives for the active dissolution of the stainless steel was calculated.

Fig. 3A shows the inhibition efficiency against inhibitor concentration. For all inhibitors, the inhibition efficiency increased with increasing the concentration and reached fast to a maximum or plateau. Similar behaviour were observed for the same compounds with carbon steel in sulfuric acid¹⁸ and other surfactants with steel in HCl¹⁹. In presence of the lowest concentration (5×10^{-5} M) maximum efficiency was 35.9 % by TMDPyBr₂, while it was 77.3 % by HMDPyBr₂ at the highest concentration (1×10^{-3} M). The results indicate two different arrangements for the inhibitors in the studied concentration range. The inhibition efficiency decreased in the order TMDPyBr₂ > MPhdPyCl₂ > HMDPyBr₂ at the low concentrations, while it decreased in the order HMDPyBr₂ > TMDPyBr₂ > MPhdPyCl₂ at the high concentrations. Fig. 3B shows the suppression efficiency against inhibitor concentration. The decreasing of i_{crit} in presence of the additives was less than that of i_{cor} but reflects significantly improvement in the passivation of the stainless steel in the acidic chloride solution. The arrangement for the efficiencies of the inhibitors in Fig. 4B is generally similar to that in Fig. 3A.

Effect of temperature: The effects of temperature on the inhibitive action of the studied inhibitors were performed. The electrochemical measurements of stainless steel were carried out in 0.1 M HCl and in absence and presence of 1×10^{-3} M inhibitor at different temperatures (30-50 °C). Firstly, it is observed that E_{cor} of the stainless steel in the pure medium increased with increasing temperature, it shifted from -508 mV at 30 °C to -480 mV at 50 °C. This is attributed to partial suppression of corrosion by accumulation of the corrosion product on the steel surface. In presence of 1×10^{-3} M inhibitor the increase of temperature didn't affect the potential, E_{cor} were

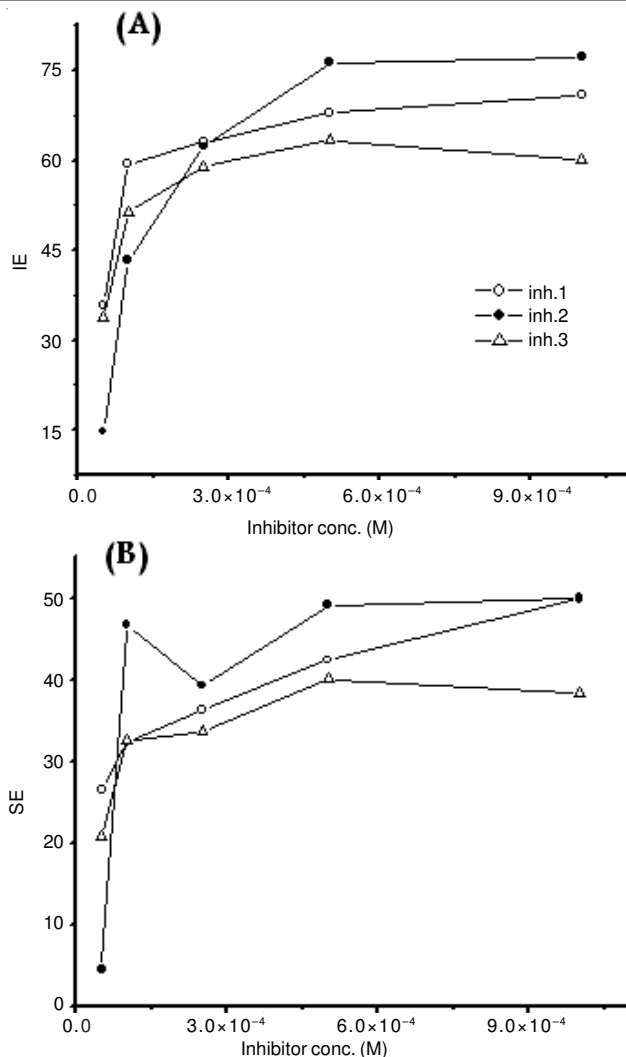


Fig. 3. Inhibition efficiency calculated from i_{cor} (A) and i_{crit} (B) against the concentration for TMDPyBr₂ (○), HMDPyBr₂ (●) and MPhdPyCl₂ (Δ)

-480, -468 and -490 mV at 30 °C and -478, -470 and -486 mV at 50 °C for TMDPyBr₂, HMDPyBr₂ and MPhdPyCl₂, respectively. This reflects a strong adsorption of the inhibitors on the stainless steel surface. The changes of the inhibition efficiency and suppression efficiency with temperature are shown in Table-2. The inhibition efficiency generally decreased with increasing temperature in presence of TMDPyBr₂ but it increased in case of HMDPyBr₂ and MPhdPyCl₂ up to maximum value at 45 °C. At this temperature the HMDPyBr₂ exerted efficiency 85 %, the highest value in this study.

The suppression efficiency, in presence of 1×10^{-3} M HMDPyBr₂, increased with increasing temperature and reached

TABLE-2
INHIBITION EFFICIENCIES (FROM TAFEL LINES AND EIS) AND SUPPRESSION EFFICIENCIES FOR THE INHIBITORS

t (°C)	TMDPyBr ₂			HMDPyBr ₂			MPhdPyCl ₂		
	IE		SE	IE		SE	IE		SE
-	Tafel	EIS	-	Tafel	EIS	-	Tafel	EIS	-
30	76.0	66.50	49.8	71.3	70.4	50.0	60	38	38.4
35	61.1	84.03	46.3	75.8	91.1	58.6	54.2	65	33.9
40	62.3	88.20	46.7	84.6	94.3	62.1	65	72.3	39.8
45	48.4	83.30	31.5	84.7	94.7	54.6	76	74.6	31.2
50	40.7	80.00	35.0	79.4	95.2	52.2	68.7	79.8	30.8

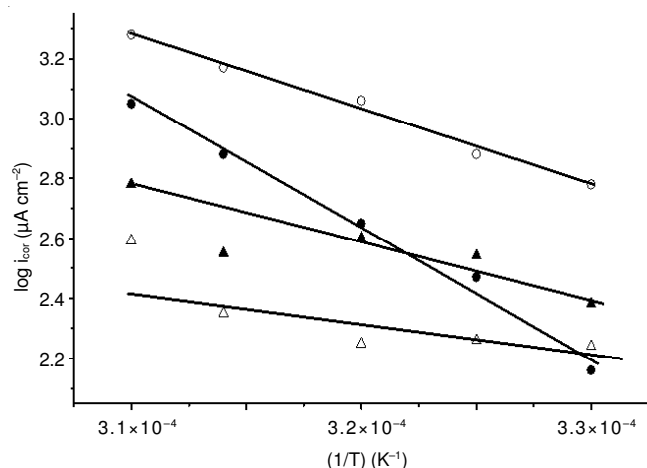


Fig. 4. Arrhenius plots for the corrosion of the SS in 0.1 M HCl (○) and in presence of 1×10^{-3} M of TMdPyBr₂ (●), HMdPyBr₂ (△) or MPhdPyCl₂ (▲)

maximum value (62.1 %) at 40 °C, as shown in Table-2. In case of TMdPyBr₂ or MPhdPyCl₂ the suppression efficiency didn't significantly influence by temperature, it decreased slightly after 40 °C. This indicates that the passivation of stainless steel is improved by these inhibitors up to 40 °C. The dependence of corrosion current density on the temperature can be expressed with Arrhenius equation:

$$\log i_{\text{corr}} = \log \lambda - \left(\frac{E_a}{2.303RT} \right) \quad (2)$$

where λ the pre-exponential factor and E_a is the apparent activation energy of the corrosion process. Plotting of $\log i_{\text{corr}}$ versus $1/T$ produced a straight line (Fig. 4). Values of E_a for stainless steel in 0.1 M HCl in the absence and presence of 1×10^{-3} M inhibitor were determined from the produced lines. The linear regression coefficients were 0.995, 0.995, 0.83 and 0.87 in case of the pure solution and in presence of TMdPyBr₂, HMdPyBr₂ and MPhdPyCl₂, respectively. The values of E_a in the pure solution and in presence of TMdPyBr₂, HMdPyBr₂ and MPhdPyCl₂ were 48.35, 82.14, 29.1 and 29.58 k J mol⁻¹, respectively. The higher value of E_a obtained in presence of TMdPyBr₂, in comparison with that of the blank solution and the general decrease of the inhibition efficiency with increasing temperature is indicative for physical adsorption (electrostatic attraction between charged molecules and the charged metal surface) of this compound. The lower values of E_a in the presence of other inhibitors and the general increase of their inhibition efficiency with increasing temperature are indicative for chemisorption (interaction of unshared electron pairs in the adsorbed molecule with the metal) on the steel surface.

Adsorption isotherm: The fraction of surface coverage (θ) by inhibitor molecules can be calculated from the equation:

$$q = \left[1 - \left(\frac{i_{\text{corr}}}{i_{\text{corr}}^0} \right) \right] \quad (3)$$

In an attempt to find the most suitable adsorption isotherm(s), θ was subjected to various adsorption isotherms. For all inhibitors, the experimental results were found to fit Langmuir isotherm for monolayer chemisorptions where θ and C (inhibitor's concentration in the bulk of the solution) are related to each other *via* the equation:

$$q = \frac{KC}{(1+KC)} \quad (4)$$

Rearrangement gives

$$\frac{C}{\theta} = \left(\frac{1}{K} \right) + C \quad (5)$$

K is the equilibrium constant of the adsorption process. Plotting of C/θ against C gives a straight line with linear regression coefficient 0.997 ± 0.001 for the three inhibitors; Fig. 5 shows the plot of MPhdPyCl₂. The slopes of the straight lines were 1.36, 1.30 and 1.60 for TMdPyBr₂, HMdPyBr₂ and MPhdPyCl₂, respectively. It is larger than one, particularly for MPhdPyCl₂, indicating the interaction between the adsorbed molecules and/or related to steric hindrance factor²⁰. The calculated K values are 1.02×10^4 , 1.43×10^4 and 2.95×10^4 for TMdPyBr₂, HMdPyBr₂ and MPhdPyCl₂, respectively. This indicating the adsorption process increased in the order TMdPyBr₂ < HMdPyBr₂ < MPhdPyCl₂.

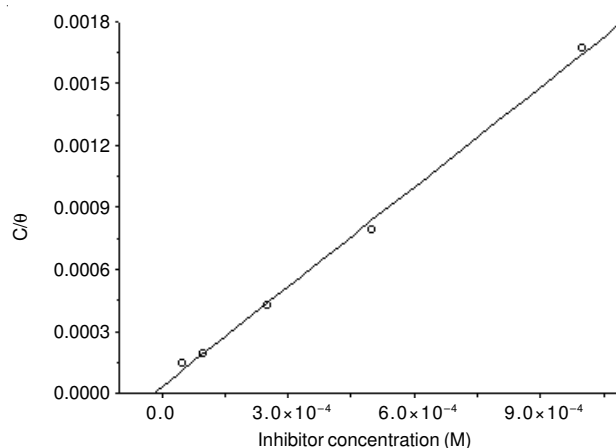


Fig. 5. Langmuir adsorption isotherm of MPhdPyCl₂ on the stainless steel surface

The constant K is related to the standard free energy of adsorption ($\Delta G_{\text{ads}}^{\circ}$) by the equation:

$$K = \left(\frac{1}{55.5} \right) \exp \left(- \frac{\Delta G_{\text{ads}}^{\circ}}{RT} \right) \quad (6)$$

where R is the gas constant and T is the absolute temperature. For the investigated inhibitors, $\Delta G_{\text{ads}}^{\circ}$ values are -33.35, -34.22 and -36.05 kJ mol⁻¹ for TMdPyBr₂, HMdPyBr₂ and MPhdPyCl₂, respectively. Generally, values of $\Delta G_{\text{ads}}^{\circ}$ around -20 kJ/mol or lower are consistent with electrostatic interaction between the charged molecules and the charged metal surface (physisorption) while those around -40 kJ/mol or higher involve charge sharing or charge transfer from the organic molecules to the metal surface to form a coordinate type bond (chemisorption)²¹. It is suggested that the chemical adsorption for the investigated inhibitors increases in the order TMdPyBr₂ < HMdPyBr₂ < MPhdPyCl₂.

Impedance measurement: Electrochemical impedance measurements were performed for 430 stainless steel in aerated 0.1 M HCl and in presence of the additives. The measurements were carried out at open circuit potential after 0.5 h of electrode immersion in which the steady state potential was established.

The electrochemical impedance spectra obtained in pure acid solution and at any studied temperature consist of two capacitive semicircles (two well-defined time-constants in Bode-phase format), large one at high and intermediate frequencies and followed by small one at low frequencies as shown in Fig. 6A. The presence of two time constants in the spectra is characteristic for rough and porous electrode or inhomogeneous film on the metal surface²². Mansfeld²³ reported that the initiation of small amounts of pits on the metal surface produces significant changes in the impedance spectra at low measured frequencies. It is explained for the spectra in Fig. 6A that the first capacitive semicircle is related to charge transfer resistance and capacity of electric double layer while the second semi-circuit is attributed to presence of pits area on the steel surface²⁴. The decrease of the diameter of the capacitive loop with increasing the temperature indicates the increase of corrosion as shown in Fig. 6A. Well fitting for these spectra, as shown in Fig. 6B, is obtained by using an equivalent circuit shown in Fig. 7A. The circuit is composed of solution resistance (R_s), capacitance of electric double layer (as constant phase element, CPE1), charge transfer resistance (R_p) and an impedance is related to pits area (consisting of capacitance, CPE2 and resistance, R).

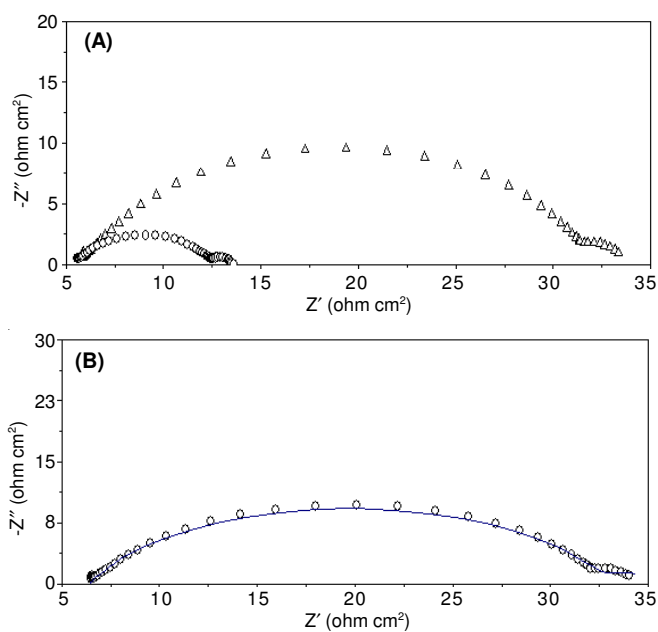


Fig. 6. (A) Nyquist plots for the corrosion of the stainless steel in 0.1 M HCl solution at 30° (Δ) and 35 °C (\circ). (B) Fitting for the spectra which recorded at 30°

In presence of the additives at 30 °C, both TMdPyBr₂ and HMdPyBr₂ produced one capacitive loop (one time-constant in Bode-phase representation), except the first concentration of TMdPyBr₂ showed second semi-circuit and the diameter of the capacitive loop increased with increasing the inhibitor concentration (Fig. 8). It is indicating that these compounds, particularly HMdPyBr₂, retarded both the general corrosion and the initiation of pitting corrosion of SS. These spectra are fitted well with the simple equivalent circuit shown in Fig. 7B.

In case of the first three concentrations of MPhdPyCl₂ electrochemical impedance spectra show two capacitive semicircles, large one and followed by very small one at low frequencies. The second semicircle disappeared in presence

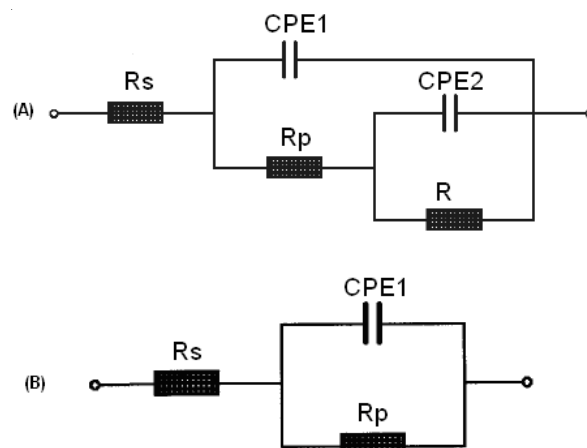


Fig. 7. Equivalent circuits represent (A) pitting corrosion model (B) general corrosion model

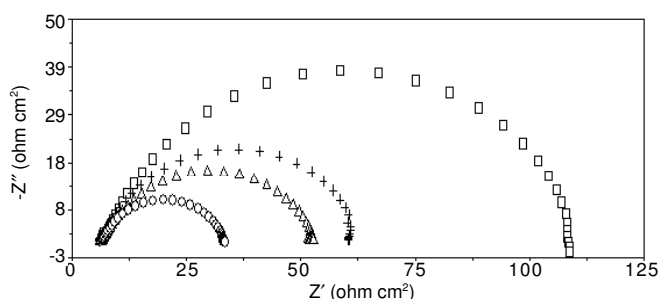


Fig. 8. Nyquist plots for the corrosion of the stainless steel in 0.1 M HCl solution containing 5×10^{-5} M (\circ), 1×10^{-4} M (Δ), 2.5×10^{-4} M (+) and 5×10^{-4} M (\square) HMdPyBr₂ at 30 °C

of the higher concentrations = 5×10^{-4} M (Fig. 9). It is indicated that this compound inhibited the general corrosion with lower efficiency than that of HMdPyBr₂ and failed to inhibit the pitting corrosion at its first concentrations. Two capacitive semicircles were obtained at OCP for iron in 1 M HCl containing phosphonium compounds which showed low inhibition or acceleration. The second semi-circuit was attributed to formation of an incomplete layer on the iron surface and this situation can lead to acceleration of the corrosion²⁵.

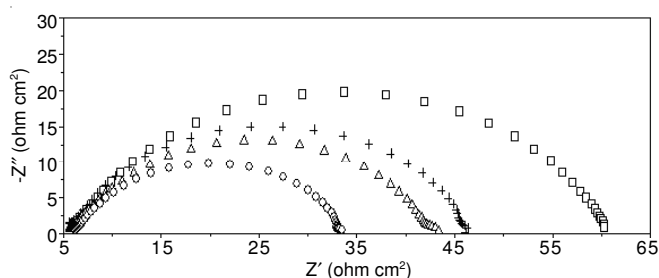


Fig. 9. Nyquist plots for the corrosion of the SS in 0.1 M HCl solution containing 5×10^{-5} M (\circ), 1×10^{-4} M (Δ), 2.5×10^{-4} M (+) and 5×10^{-4} M (\square) MPhdPyCl₂ at 30 °C

At 1×10^{-3} M both TMdPyBr₂ and HMdPyBr₂ gave one capacitive loop while MPhdPyCl₂ gave two capacitive loops in all measurements at higher temperatures (35-50 °C). This confirmed the good inhibition by TMdPyBr₂ and HMdPyBr₂ and the weak role of MPhdPyCl₂ against the initiation of pitting corrosion in the aggressive condition. Fig. 10 shows representative electrochemical impedance spectra of the three

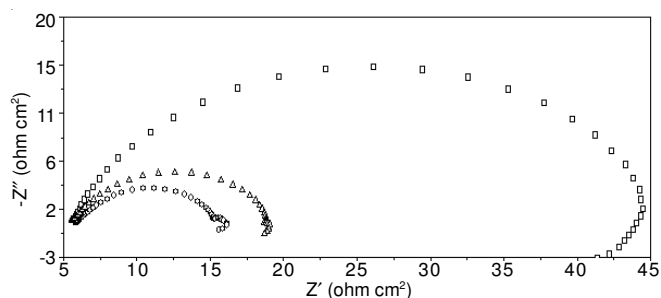


Fig. 10. Nyquist plots for the corrosion of the SS in 0.1 M HCl solution containing 1×10^{-3} M of MPhdPyCl₂ (○), TMdPyBr₂ (Δ) and HMdPyBr₂ (□) at 50 °C

inhibitors at 50 °C. An inductive loop is appeared at low frequency region in the spectra of all the investigated compounds. This has been determined for iron-based materials at E_{cor} in acid media in the presence of inhibitors²⁶.

Fig. 11 shows the inhibition efficiency calculated from R_p values against the concentration for the three inhibitors at 30 °C. Generally, there is agreement with that calculated from corrosion current (Fig. 3A). The maximum efficiency by HMdPyBr₂ was 76.6 % in presence of 5×10^{-4} M while by using polarization measurement it was 77.3 % in presence of 1×10^{-3} M. The inhibition efficiency calculated from electrochemical impedance at different temperature (Table-2) are also in agreement with the polarization results. HMdPyBr₂ exhibited best inhibition efficiency among the studied compounds. There was general increasing of inhibition efficiency with temperature in presence of HMdPyBr₂ and MPhdPyCl₂ and reach the maximum values 95.2 and 79.8 %, respectively, at 50 °C (84.7 and 76 %, respectively, at 45 °C by polarization measurement), respectively. These results confirm the chemisorption behaviour of these compounds. TMdPyBr₂ shows maximum efficiency (88.2 %) at 40 °C, the difference in its result from that by polarization measurement reflects that this compound is acted by physical and weak chemical adsorption.

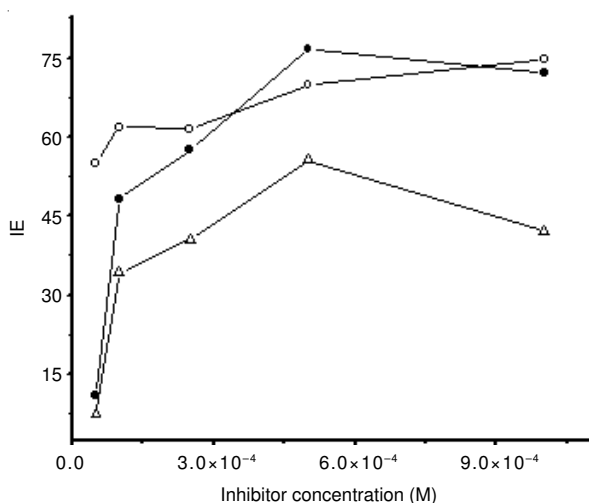


Fig. 11. Inhibition efficiency calculated from R_p against the concentration for TMdPyBr₂ (○), HMdPyBr₂ (●) and MPhdPyCl₂ (Δ)

Microscopic study: Microscopic investigation of the steel surface after 0.5 h immersion in 0.1 M HCl solution at 45 °C in absence and presence of 1×10^{-3} M additives are shown in

Fig. 12. It is clear that the stainless steel suffered from general and localized attack (image A) and the presence of TMdPyBr₂ (image B) or HMdPyBr₂ (images C) protected well the stainless steel surface. MPhdPyCl₂ couldn't protect the stainless steel completely, some local attack is observed in the image D. This result is in quite reasonable agreement with the result of electrochemical methods.

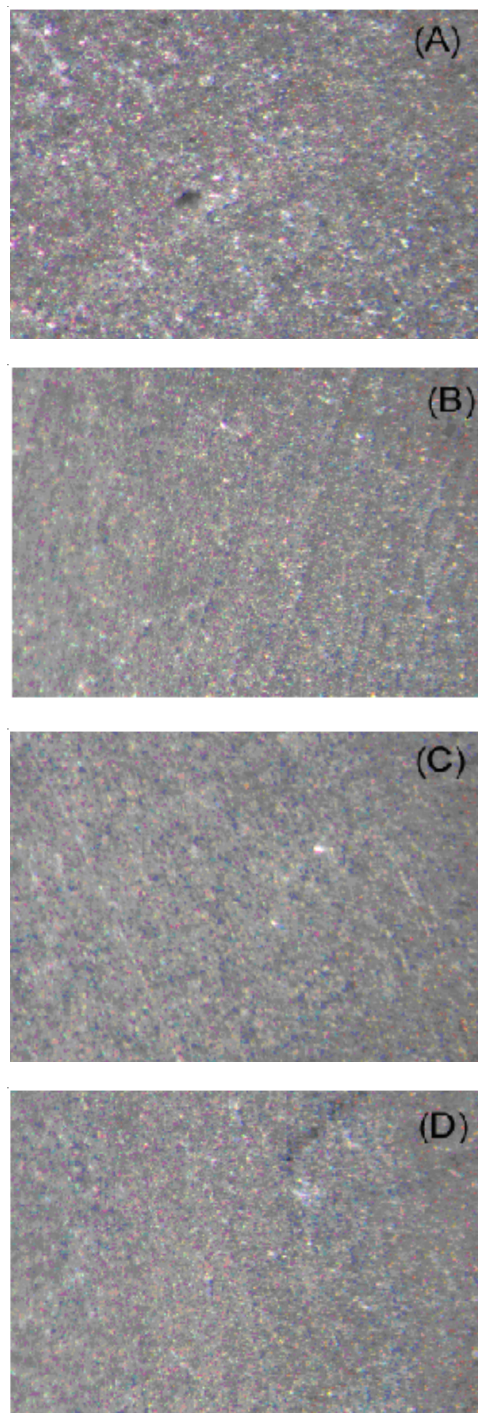


Fig. 12. Microscopic images after immersion of the SS in 0.1 M HCl solution in absence (A) and presence of 1×10^{-3} M TMdPyBr₂ (B), HMdPyBr₂ (C) and MPhdPyCl₂ (D) at 45 °C

Mechanism of inhibition: Adsorption process occurs by electrostatic forces between ionic charges or dipoles of the adsorbed species and the electric charge on the metal surface

which can be expressed by its potential with respect to potential of zero charge (pzc). Also, the inhibitor molecules can be adsorbed onto the metal surface *via* the electron transfer from the adsorbed species to the vacant electron orbital of low energy in the metal to form a coordinate type of link¹¹. It was explained that the surfactant molecules adsorb by its head (hydrophilic) directing its tail (hydrophobic) to the solution face leading to decrease in the corrosion rate^{12,27}. It is suggested that the two ammonium groups and aromatic rings in the dipyridinium molecule can be adsorbed at the different sites on the metallic surface. The molecule is physically adsorbed *via* the two positively charged nitrogen atoms and the aromatic rings are parallel to the surface and the methyl group tail is extended away in the solution. This position is allowed for transfer of the π -electrons of the pyridine rings to the vacant electron orbital of low energy in the metal to form a coordinate type of link (chemical adsorption)¹⁸. The transformation from physical adsorption to chemical type can be occurred gradually²⁸.

Delocalization of π orbital in the pyridine ring may increase the positive charge on the nitrogen atom of the ring. In other side, the attached methyl groups increase the electron density of the aromatic rings while they may decrease the positive charge of the nitrogen atom. In other words, the attached methyl groups increase the chemisorption property of the dipyridinium molecule. Many arguments in this study prove that the higher methylated molecule HMdPyBr₂ has strong chemisorption with the stainless steel surface while the lower methylated molecule TMdPyBr₂ is acted by weaker chemical adsorption. The chemisorption type inhibitor is important for protection of the stainless steel particularly in aggressive solutions containing chloride ions. The blocking of the active sites on the surface by strong chemical adsorption of the inhibitor enhances the oxide film formation.

The chemical structure of MPhdPyCl₂ molecule is different (Fig. 1) by presence of two methyl phenyl groups attached to the nitrogen atom. The presence of additional two benzene rings is expected to increase the covered area and the electronic interaction with the metal surface. MPhdPyCl₂ caused low corrosion activation energy than that in pure medium and had largest K value and largest negative $\Delta G^{\circ}_{\text{ads}}$ value among the investigated compounds, indicating strong chemisorption of this compound. In our previous work¹⁸ MPhdPyCl₂ exhibited highest inhibition efficiency, among the same group inhibitors, for low carbon steel in H₂SO₄ solution. However, in this study, this inhibitor showed the lowest inhibition efficiency of stainless steel in HCl solution and weak inhibitor for pitting initiation. At higher concentration of this inhibitor a red-brown precipitate is formed on the steel surface at the open circuit potential as observed before¹⁸. This inhibitor, most likely, is exposed to irreversible reduction and deposited as precipitate on the electrode surface. Although the deposited layer enhanced the inhibition (secondary inhibition) of mild steel in sulfuric, it is inefficient against the pitting corrosion of the stainless steel. The secondary inhibition may be higher or lower than primary inhibition, depending on the effectiveness of the reaction products²⁹.

In this study HMdPyBr₂ is superior inhibitor among the studied compound for both the general and localized corrosion of stainless steel in HCl solution. However, this compound

exhibited least inhibition efficiency for corrosion of mild steel in H₂SO₄ and it was attributed to influence of steric hindrance of the attached methyl groups on the adsorption of the molecule¹⁶. But, why the steric hindrance doesn't influence in the stainless steel-HCl system. This is explained by the fact that the changes of the substrate metal and/or the type of aggressive electrolyte are significantly influenced on the adsorption process of the same inhibitor²⁹.

Conclusion

The used dipyridinium salts work as mixed type inhibitors with dominant anodic against the corrosion of the stainless steel in 0.1 M HCl solution. They do not alter the mechanism of either hydrogen evolution or steel dissolution reactions. The values of E_a in absence and presence of TMdPyBr₂, HMdPyBr₂ and MPhdPyCl₂ were 48.35, 82.14, 29.1 and 29.58 kJ mol⁻¹, respectively. The adsorption of these compounds on the steel surface was found to obey Langmuir adsorption isotherm. The calculated K values were 1.02×10^4 , 1.43×10^4 and 2.95×10^4 and $\Delta G^{\circ}_{\text{ads}}$ values were -33.35, -34.22 and -36.05 kJ mol⁻¹ for TMdPyBr₂, HMdPyBr₂ and MPhdPyCl₂, respectively. These arguments suggested that the chemical adsorption for the investigated inhibitors increases in the order TMdPyBr₂ < HMdPyBr₂ < MPhdPyCl₂. However, the inhibition efficiency and suppression efficiency increased in the order MPhdPyCl₂ < TMdPyBr₂ < HMdPyBr₂. The appearance of second capacitive semicircle in the low frequencies region of the Nyquist plot was attributed to presence of pits on the steel surface. Both TMdPyBr₂ and HMdPyBr₂ inhibit the pitting initiation while MPhdPyCl₂ is less efficient inhibitor against the pitting. The optical microscopic investigation is in quite reasonable agreement with the result of electrochemical methods. The superiority for HMdPyBr₂ as inhibitor was attributed to the higher attached methyl groups which increase the chemisorption property of the dipyridinium molecule. In spite of its chemisorption on the stainless steel surface, MPhdPyCl₂ showed the lowest inhibition efficiency. This inhibitor, most likely, is exposed to irreversible reduction and deposited as precipitate on the electrode surface.

ACKNOWLEDGEMENTS

The authors are grateful to Saudi Basic Industries Corporation (SABIC) and to the Research and Development Center in the King Abdulaziz University under contract No. MS/9/4 for financial support of this work.

REFERENCES

1. J.W. Schultze and M.M. Lohrengel, *Electrochim. Acta*, **45**, 2499 (2000).
2. H.M. El-Kashlan, *Asian J. Chem.*, **23**, 5235 (2011).
3. T. Yanardag, S. Özbay, S. Dincer and A.A. Aksüt, *Asian J. Chem.*, **24**, 47 (2012).
4. S.A.M. Refaey, F. Taha and A.M. Abd El-Malak, *Appl. Surf. Sci.*, **242**, 114 (2005).
5. F. Bentiss, M. Lagrenee, M. Trainsel and J.C. Hornez, *Corros. Sci.*, **41**, 789 (1999).
6. A. Popova, M. Christov and A. Vasilev, *Corros. Sci.*, **49**, 3276 (2007).
7. A. Popova, M. Christov and A. Vasilev, *Corros. Sci.*, **49**, 3290 (2007).
8. M.S. Abdel-Aal, M. Th. Makhlof and A.A. Hermas, Proceedings of The Seventh European Symposium on Corrosion Inhibitor, Ann. Univ. Ferrara, N.S. sezV, Suppl. No. 9, p. 1143 (1990).
9. M.H. Wahdan, A.A. Hermas and M.S. Morad, *Mater. Chem. Phys.*, **76**, 111 (2002).

10. A.A. Hermas, M.S. Morad and M.H. Wahdan, *J. Appl. Electrochem.*, **34**, 95 (2004).
11. M.A. Migahed, *Mater. Chem. Phys.*, **93**, 48 (2005).
12. M.M. Saleh, *Mater. Chem. Phys.*, **98**, 83 (2006).
13. M. El Achouri, S. Kertit, H.M. Goultaya, B. Nciri, Y. Bensouda, L. Perez, M.R. Infante and K. Elkacemi, *Prog. Org. Coat.*, **43**, 267 (2001).
14. M. El Achouri, M.R. Infante, F. Izquierdo, S. Kertit, H.M. Goultaya and B. Nciri, *Corros. Sci.*, **43**, 19 (2001).
15. P. Stipa, *Spectrochim. Acta A*, **64**, 653 (2006).
16. J.-Y. Ock, H.-K. Shin, Y.-S. Kwon and J. Miyake, *Colloid. Surf. A*, **257-258**, 351 (2005).
17. S.G. Aziz, A.Y. Obaid, A.O. Alyoubi and A.A. Abdel Fattah, *Corros. Preven. Control*, **44**, 179 (1997).
18. M.S. Morad, A.A. Hermas, A.Y. Obaid and A.H. Qusti, *J. Appl. Electrochem.*, **38**, 1301 (2008).
19. S.Z. Yao, X.H. Jiang, L.M. Zhou, Y.J. Lv and X.Q. Hu, *Mater. Chem. Phys.*, **104**, 301 (2007).
20. M.S. Morad, *J. Appl. Electrochem.*, **29**, 619 (1999).
21. M. Lebrini, M. Lagrenee, H. Vezin, M. Traisnel and F. Bentiss, *Corros. Sci.*, **49**, 2254 (2007).
22. T. Hong and W.P. Jepson, *Corros. Sci.*, **43**, 1839 (2001); M.C. Li, C.L. Zeng, S.Z. Luo, J.N. Shen, H.C. Lin and C.N. Cao, *Electrochim. Acta*, **48**, 1735 (2003).
23. F. Mansfeld, *Electrochim. Acta*, **35**, 1533 (1990).
24. H. Shih and F. Mansfeld, *Corrosion*, **45**, 610 (1989).
25. K.F. Khaled, *Appl. Surf. Sci.*, **230**, 307 (2004).
26. F. Mansfeld, An Introduction to Electrochemical Impedance Measurement, Technical Report No. 26, Part No.: BTR026, Solartron Limited, May, pp. 1-14 (1999).
27. R. Zyauya and J.L. Dawson, *J. Appl. Electrochem.*, **24**, 943 (1994).
28. S.A. Abd El-Maksoud and A.S. Fouda, *Mater. Chem. Phys.*, **93**, 84 (2005).
29. G. Trabaneli, In ed.: F. Mansfeld, Corrosion Inhibitors, in Corrosion Mechanisms, Marcel Dekker, Inc. New York, p. 119 (1989).